XXVI Simpósio Brasileiro de Recursos Hídricos
23 a 28 de novembro de 2025 - Vitória - ES

ABRHidro
Associação Brasileira de Recursos Hídricos

XXVI SIMPÓSIO BRASILEIRO DE RECURSOS HIDRÍCOS

EFFECTS OF PERIODIC WIND FORCING ON INTERNAL SEICHES OVER SLOPED TOPOGRAPHY

Rafael de Carvalho Bueno[1]; Tobias Bleninger[2] & Andreas Lorke[3]

Abstract: Internal waves are critical drivers of mixing and ecological dynamics in stratified lakes. While wind-forced internal seiches are well studied, the role of wind periodicity in modulating basin-scale hydrodynamics remains unclear. Through a series of non-hydrostatic numerical simulations in idealized two-dimensional basins, we show that the ratio between the wind forcing period (σ_f) and the fundamental internal seiche period (T_{V1H1}) plays a pivotal role in shaping boundary layer dynamics and energy dissipation processes. Our results reveal that for $\sigma_f/T_{V1H1} > 1$, the system exhibits enhanced bottom boundary layer (BBL) separation and offshore-directed turbulent jets, promoting elevated turbulent kinetic energy (TKE) dissipation rates, up to three times higher than under supercritical conditions. This regime supports non-resonant forced waves modulated and sustained re-energization of basin circulation and BBL separation. Conversely, when $\sigma_f/T_{V1H1} < 1$, BBL separation is inhibited, and the system transitions to a regime dominated by propagating waves that can shoal and break near sloping topography.

Keywords: Lake circulation, Thermal stratification, Numerical modeling, Nonhydrostatic simulation

INTRODUCTION

Hydrodynamic processes play a critical role in shaping ecological dynamics in lakes and reservoirs. Internal wave, which is an oscillatory motion within stratified water layers (Mortimer, 1952), rank among the most ecologically significant hydrodynamic phenomena. These waves enhance turbulent mixing in both pelagic and littoral zones (Cossu & Wells, 2013; de Carvalho Bueno et al., 2023a), modulate light penetration (Hingsamer et al., 2014), drive sediment resuspension and transport (Valipour et al., 2017), and influence dissolved oxygen dynamics (Amitai et al., 2024; Flood et al., 2021; Valerio et al., 2019). Furthermore, internal waves exert direct control on phytoplankton and cyanobacteria communities (Chowdhury et al., 2016; Hingsamer et al., 2014; Pannard et al., 2011; Plisnier et al., 2023) and impact fish abundance in lakes (Jarić et al., 2022; Plisnier et al., 2023).

Internal seiches represent a particularly significant class of internal waves for driving large-scale circulation in closed basins such as lakes and reservoirs. These standing waves develop when sustained wind forcing establishes sufficient shear stress at the water surface to reach steady-state conditions. Their dynamics are governed by multiple factors including stratification profile, wind resonance, Coriolis effects, and basin morphology and topography.

Numerical simulations demonstrate that sloping topography play a critical role on internal seiche damping, facilitating energy transfer from basin-scale oscillations to localized littoral mixing (de Carvalho Bueno et al., 2023b). This energy redistribution fundamentally alters circulation

1) Post-graduate Program of Environmental Engineering, Federal University of Paraná, Brazil, e-mail: rafael.bueno@ufpr.br
2) Department of Environmental Engineering, Federal University of Paraná, Brazil, e-mail: bleninger@ufpr.br
3) Institute for Environmental Sciences, University of Kaiserslautern-Landau, Germany, e-mail: lorke@uni-landau.de

patterns compared to systems where seiches persist with minimal dissipation (Lemmin, 1987). Theoretical analyses reveal that sloping topography substantially modifies internal seiche damping rates and consequent circulation dynamics (Figure 1a). Recent advances have identified the *wave attractor number* (A_t) as a key dimensionless parameter governing seiche damping (de Carvalho Bueno et al., 2024, 2025). This parameter quantifies the relationship between internal wave propagation direction and bottom slope (Henderson & Deemer, 2012). In subcritical regime ($A_t < 1$; Figure 1b), post-upwelling relaxation generates intrusive gravity currents through bottom boundary layer separation (de Carvalho Bueno et al., 2025; Nielson & Henderson, 2023). These processes disrupt thermal stratification, enhance localized turbulent mixing, and drive cross-slope transport, effectively redistributing boundary water masses into the pelagic zone (Figure 1).

Figure 1. Schematic representation of gentle topography effects on internal seiche damping (de Carvalho Bueno et al., 2025). a) Longitudinal lake cross-section showing bottom boundary layer (BBL) separation dynamics. The upward arrow represents the internal seiche-induced upwelling, and the downward arrow illustrates the downslope-propagating front returning to equilibrium. Their interaction triggers BBL separation, generating a metalimnion intrusion (red arrow). b) Illustrate the relationship between the wave attractor number (A_t) and internal seiche amplitude, highlighting the conditions under which the mechanism described in (a) is most likely to occur. A_t, a function of basin slope, regulates internal wave energy focusing definition (see de Carvalho Bueno et al. (2025) and Nielson & Henderson (2023) for formal definition).

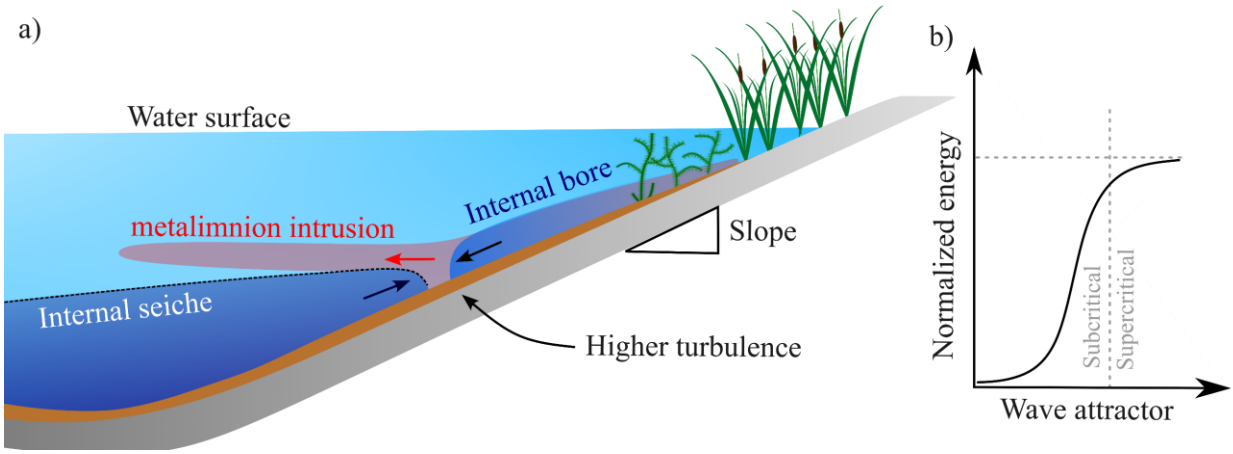

This process (Figure 1a) has been recently documented through field measurements in Lacamas Lake (Nielson & Henderson, 2023) and systematically evaluated from numerical modeling for different sloping conditions (de Carvalho Bueno et al., 2025). The numerical study, employing single-pulse wind forcing, revealed that sloping topography is the primary driver of bottom boundary layer separation and subsequent circulation pattern modifications. However, in natural systems, wind forcing is typically periodic, governed by diurnal and semi-diurnal atmospheric cycles. Resonance between internal seiches and wind-forced oscillations has been widely observed across different lakes (Antenucci & Imberger, 2003). While diurnal and semi-diurnal wind components are often predominant, dominant wind forcing frequencies vary widely among lakes (Laval et al., 2003). Laboratory experiments demonstrate that wind forcing periods exceeding the period of fundamental internal seiche generate forced seiche responses, whereas shorter wind periods excite internal seiche with higher horizontal modes (Boegman & Ivey, 2012).

Despite robust evidence for periodic wind effects on internal waves (Antenucci & Imberger, 2003; Bernhardt & Kirillin, 2013; Valerio et al., 2019), most studies remain site-specific and rarely address how periodic winds interact with sloping topography. Although limited evidence suggests

wind resonance may sustain nearshore mixing through energy dissipation cycles, analogous to single-pulse dynamics (de Carvalho Bueno et al., 2025), these mechanisms remain poorly investigated.

This study aims to investigate how periodic wind forcing influences internal seiche dynamics and circulation patterns in lakes with sloping topography. Through three-dimensional non-hydrostatic numerical simulations, we analyzed the physical mechanisms governing wind-driven internal seiches under periodic forcing conditions.

METHODS

Numerical experiments

The influence of periodic wind forcing on the damping of internal seiches over sloping topography was investigated using Delft3D, a three-dimensional hydrodynamic model with a nonhydrostatic solver. The study analyzed the internal seiche response, characterized by temperature distribution, horizontal velocities, and energy dissipation rates, induced by wind events over a five-day simulation period. 6 simulations were conducted, varying the slope topography and wind patterns to assess how periodic wind influences lake circulation under different topographic regimes (Figure 1b). The slope topography was defined based on the wave attractor ratio (A_t), considering two cases: A_t=15.91 (Case 1; Supercritical regime) and A_t=0.35 (Case 2; Subcritical regime). All simulations were conducted on a 10 m deep and 500 m wide reservoir-shaped channel with an effective length (L_e) of 10 km (Figure 2).

Figure 2. Schematic cross-section of the basin geometry used in numerical experiments. Different shades of blue represent the epilimnion and hypolimnion. h_e denotes the epilimnion thickness, while ρ_e and ρ_h correspond to the water densities of the epilimnion and hypolimnion, respectively. L_1 and L_2 represent the surface lengths of the basin for Case 1 ($A_t = 0.35$; Slope 1 = 0.0011) and Case 2 ($A_t = 15.91$; Slope 2 = 0.05), respectively, while L_e is the effective basin length at the thermocline depth. Apart from L_1 and L_2, and the differences in slope, all other parameters shown in the figure are identical for both cases. The red vertical dashed line marks the location where wave amplitude was evaluated.

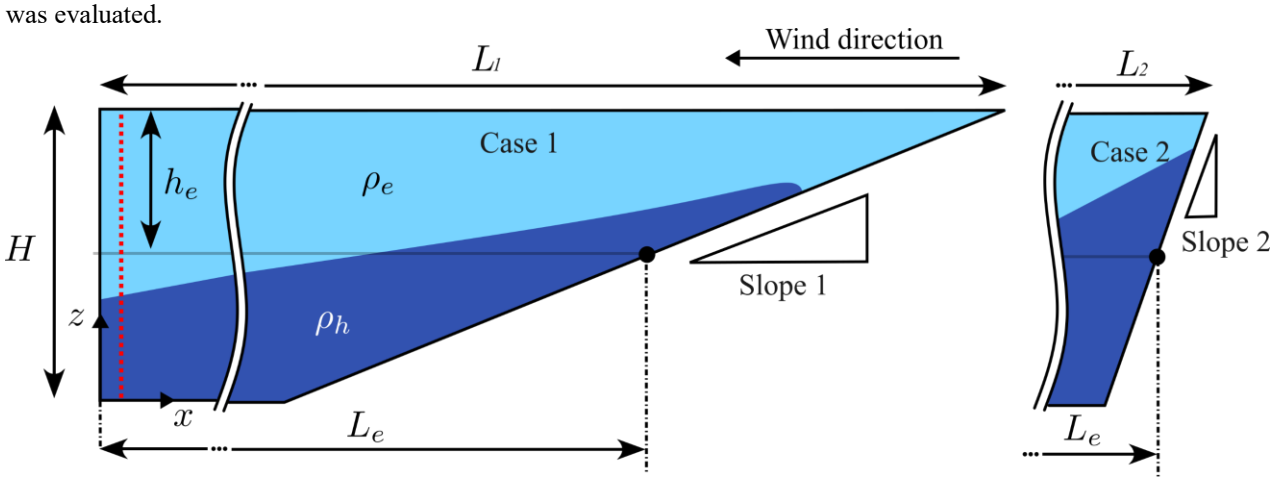

The reservoir was bounded by a straight vertical wall at one end and a sloping bottom at the opposite side. Stratification followed a two-layer system with an 8 °C temperature difference, where the epilimnion remained at 28 °C, and the thermocline (h_e) was positioned at a depth of 5 m. According to the basin characteristics and stratification condition, the fundamental internal seiche period (T_{V1H1}) was approximately 15 h. Although this study considers a specific set of conditions, previous numerical investigations have shown that internal seiche damping over sloping topography can be generalized using the wave attractor ratio A_t (de Carvalho Bueno et al., 2025), which accounts for variations in lake size and wind intensity. The two sets of numerical experiments conducted in this study represent distinct dynamical regimes characterized by the wave attractor ratio (Figure 2;

case 1 vs case 2). In the supercritical regime ($A_t > 1$; case 2), the influence of sloping topography on internal seiche damping is expected to be negligible (de Carvalho Bueno et al., 2025). In contrast, according to previous investigations, the subcritical regime ($A_t < 1$; case 1) exhibits strong interactions between internal waves and the bottom slope, leading to boundary layer separation, rapid wave damping, and a localized increase in turbulent kinetic energy (TKE) dissipation rates (de Carvalho Bueno et al., 2025).

In all simulations, the water was initially at rest before being exposed to a maximum wind speed of 5 m/s, directed toward the basin end opposite the sloping bottom. This wind intensity was chosen to ensure conditions favorable for the dominance of internal seiches (Spigel & Imberger, 1980), like those found in Lake Tahoe (Roberts et al., 2021), Kootenay Lake (Stevens & Lawrence, 1997), and Lake Erie (Lin et al., 2021). While wind duration varied across simulations, a minimum wind period of 3h was defined in all cases to have conditions favorable to maintain a steady-state circulation (Dorostkar & Boegman, 2013; Stevens & Imberger, 1996). For each case (Figure 2), three simulations were conducted under distinct wind forcing regimes. One set employed a single 8-hour wind pulse, consistent with previous numerical experiments (de Carvalho Bueno et al., 2025). The other simulations applied periodic wind forcing with two different periodicities (σ_f): 5 h ($\sigma_f \ll T_{V1H1}$) and 30 h ($\sigma_f \gg T_{V1H1}$). In all periodic cases, wind forcing began with a constant wind speed of 5 m/s applied for the initial 5 hours of simulation (Figure 3). These scenarios were designed to explore the internal seiche response across a range of forcing frequencies relative to the fundamental internal seiche period (Boegman & Ivey, 2012).

Figure 3. Wind forcing illustrates the first 40 hours of simulation. a) Time series and b) power spectral density (PSD) of wind speed applied to numerical experiments. The dashed lines indicate the mean red noise spectrum for the time series at a 95% confidence level. The vertical red dashed line shows the fundamental internal seiche period of all numerical experiments (15h).

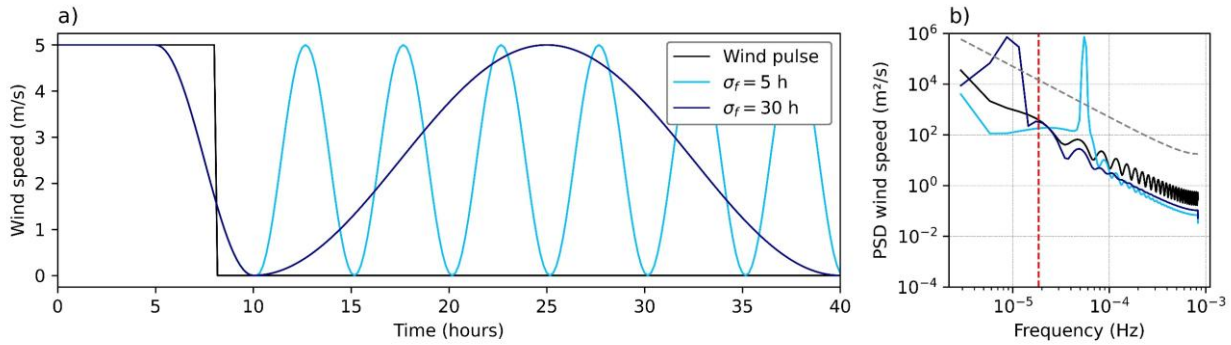

Numerical model

Internal seiches in thermally stratified lakes have been widely simulated using hydrodynamic models (Hodges et al., 2000; Marti & Imberger, 2006; Vilhena et al., 2013). In this study, we employed the three-dimensional Delft3D-FLOW model with a non-hydrostatic solver to better capture internal seiche degeneration (Wadzuk & Hodges, 2009). The model is based on the Reynolds-averaged Navier-Stokes equations and the Boussinesq approximation for incompressible flows (Deltares, 2014), while neglecting Coriolis effects. It solves the three-dimensional governing equations for mass, heat, and momentum. The model was configured using a rectangular grid with a horizontal resolution of 10 m and a vertical resolution of 12.5 cm, meeting the minimum requirements for the non-hydrostatic solver to reproduce non-hydrostatic effects (Wadzuk & Hodges, 2009).

The turbulence was modeled using k-ε turbulence closure model, with background vertical eddy viscosity and eddy diffusivity treated as calibration coefficients to account for dissipation and

mixing due to unresolved flows. The surface boundary condition was defined by a time series of wind shear stress, computed using the bulk aerodynamic formulation with a wind drag coefficient of 2.0×10^{-3}, on the constant wind speed range applied in the simulations (Wüest & Lorke, 2003). Heat exchange at the surface was neglected, assuming no significant variation in thermal stratification affecting the internal seiche structure over the 5-day simulation period. Bottom shear stress was modeled using the Manning formulation, with a constant roughness coefficient of 0.035. The temporal resolution was set to 0.6 s to ensure numerical stability. Additional details on the numerical and physical parameters used in these simulations can be found in de Carvalho Bueno et al. (2025), which employed similar numerical experiments.

Hydrodynamic Analysis

The results were analyzed based on the time-series of vertical distribution of temperature, and turbulent kinetic energy dissipation rates along a longitudinal transect at the basin center ($y = 250$ m). The internal wave oscillation was characterized by the deviation between the temporally averaged thermocline depth and its vertical excursion, evaluated on the side of the basin opposite to the sloping topography (Figure 2, red dashed line). The wave amplitude was determined at the point of maximum displacement, defined as the location where the first temporal derivative of the thermocline depth is zero. To identify dominant periods of internal wave oscillations, time series data were analyzed using spectral analysis based on Welch's method (Welch, 1967), employing a Hamming window. Significant peaks in the power spectral density were identified by comparing the spectra against a red noise background spectrum at the 95% confidence level (de Carvalho Bueno et al., 2020).

To evaluate the impact of periodic wind forcing and sloping topography on lake mixing dynamics, turbulent kinetic energy dissipation rates were integrated vertically and longitudinally.

RESULTS

Consistent across all simulations, persistent wind forcing effectively transferred momentum at the water surface, driving energy downward across the surface boundary layer (SBL). This energy input strengthened horizontal pressure gradients, accelerating the hypolimnetic water in the upwind direction. The baroclinic response manifested as distinct thermocline upwelling along the sloping topography, with compensatory downwelling developing on the opposing basin side.

In the supercritical regime (Case 2), where the bottom slope exceeded the critical wave slope, the inertial response of displaced water generated persistent oscillatory motion around nodal points, sustaining the internal seiche even after the wind ceases (Figure 4a). The 5-hour wind pulse generated an internal seiche with 15-hours period (Figure 4b) and maximum amplitude of approximately 2 m (Figure 4a). Under these conditions, energy dissipation was primarily governed by bottom shear stress near wave nodes, where kinetic energy became concentrated (Figure 4c).

In contrast to case 2 numerical experiment, results under subcritical conditions (Case 1) exhibited partial suppression of internal seiche generation due to gentle sloping topography (Figure 4a). Approximately 95% of energy dissipation was released during the initial seiche formation phase, with maximum dissipation rates occurring within the first 24 hours of simulation as the thermocline-topography interaction developed (Figure 4c). The interaction enhanced turbulent kinetic energy (TKE) dissipation rates by approximately threefold compared to supercritical conditions, with peak dissipation occurring during the second half of the first wave cycle.

Wind-driven surface stress displaced hypolimnetic water toward the leeward shore, forcing upslope propagation of the water mass. Simultaneously, deeper hypolimnetic layers developed a restoring flow toward equilibrium, maintaining oscillatory motion. Although this initial interaction

could theoretically attenuate wave energy, most of the energy remained preserved (Figure 4a). The dominant energy dissipation occurred during the second half of the first wave cycle, when residual seiche energy generated a new upslope front that collided with the returning downslope flow. This interaction triggered bottom boundary layer (BBL) separation, substantially enhancing energy dissipation through the formation of a turbulent intrusion jet, as the mechanism illustrated in Figure 1 and detailed described in previous studies (de Carvalho Bueno et al., 2025).

Figure 4. Internal seiche dynamics and turbulent kinetic energy (TKE) dissipation during a single wind event under subcritical and supercritical topographic regimes. a) Time series and b) power spectral density (PSD) of internal wave oscillations measured at the side of the basin opposite the sloping topography (Figure 2, red dashed line). The gray box indicates the total duration of the wind event. In b) the dotted line represents the mean red noise spectrum at the 95% confidence level, while the vertical red dashed line shows the theoretical fundamental internal seiche period of these simulations. c) Time-series of integrated TKE dissipation. Shades of red indicate periods when dissipation is higher in the subcritical regime, whereas shades of blue correspond to periods of greater dissipation in the supercritical regime. The dotted line indicates the wave amplitude at the side of the basin opposite the sloping topography for supercritical condition.

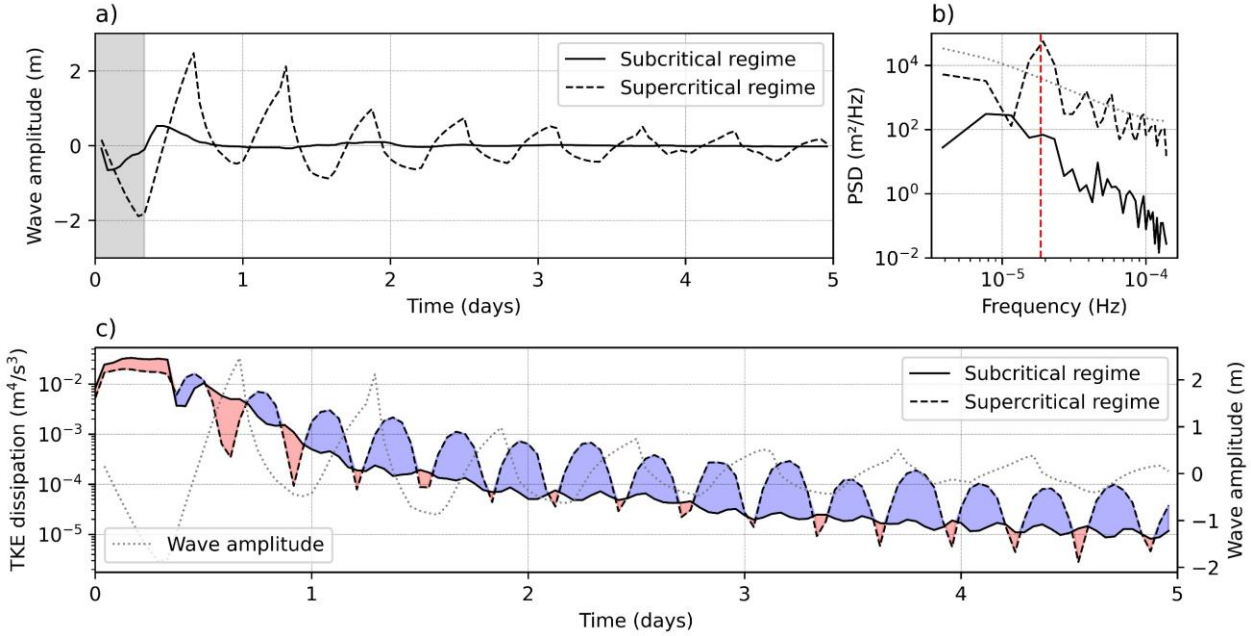

Numerical simulations under supercritical conditions and periodic wind forcing revealed two distinct hydrodynamic regimes, controlled by the ratio between the wind forcing period (σ_f) and the period of fundamental internal seiche (T_{V1H1}). In simulations with σ_f=5 h ($\sigma_f < T_{\mathrm{V1H1}}$), higher-mode internal seiches were generated (Figure 5a), whereas a longer forcing period (σ_f=30 h; $\sigma_f > T_{\mathrm{V1H1}}$) led to the development of non-resonant, forced internal seiches with wave period matching the wind forcing period. In both cases, the response was modulated by a low-amplitude fundamental internal seiche, as indicated by spectral analysis (Figure 6b–d; gray line). TKE dissipation was predominantly driven by wind shear in the surface boundary layer during active forcing, accounting for 98% of total dissipation, while bottom shear contributed only 2% during wave evolution. Under calm wind conditions, the highest dissipation rates occurred near the nodes of basin-scale internal waves, where kinetic energy was most concentrated.

In subcritical regimes, simulations with extended wind forcing periods (σ_f=30 h > T_{V1H1}) generated forced non-resonant internal seiches while completely suppressed the development of the fundamental internal seiche. The flow dynamics were dominated by cyclic BBL separation events, triggered by interactions between upslope-propagating fronts and returning downslope flows. These

interactions produced offshore-directed turbulent jets and increased the integrated TKE dissipation rates by a factor of three compared to supercritical conditions (Figure 6), reaching magnitudes similar to those observed in single wind-pulse simulations (Figure 4c). As most of the seiche energy was dissipated through these repeated interactions, the formation and propagation of a coherent fundamental internal seiche were effectively inhibited (Figure 6d). In contrast to supercritical conditions, where only 2% of the dissipated energy was not associated with wind shear in the SBL, the subcritical regime exhibited over 15% of total energy dissipation during calm periods, primarily driven by BBL separation processes at sloping topography.

Figure 5. North–south velocity component along the longitudinal transect from the numerical simulation forced with a 5-hour periodic wind (σ_f=5 h) for a) supercritical and b) subcritical conditions.

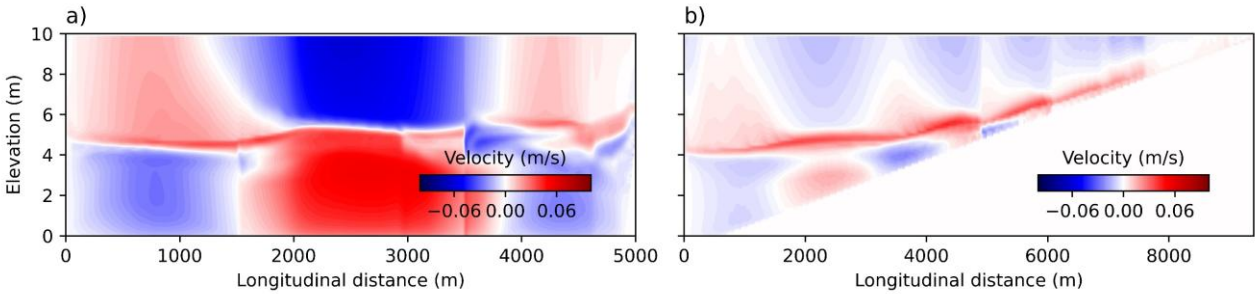

While subcritical regime simulations with extended wind forcing periods (σ_f=30 h > T_{V1H1}) triggered persistent BBL separation, experiments with shorter forcing periods (σ_f= 5 h) exhibited fundamentally different dynamics compared to their supercritical counterparts. Instead of generating higher-mode internal seiches, as observed under supercritical conditions (Figure 5a), the subcritical system subjected to σ_f= 5 h forcing produced high-frequency internal waves that continuously propagated along the sloping topography (Figure 5b). This wave propagation regime effectively suppressed both the development of internal seiches and the BBL separation typically associated with single wind-pulse events. Although these high-frequency waves could enhance nearshore TKE dissipation relative to other subcritical cases, the overall dissipation rates remained comparable to those in supercritical simulations, with less than 10% variation.

DISCUSSION

We examined the effects of periodic wind forcing on lake circulation and mixing by analyzing the hydrodynamic processes governing internal wave oscillations and turbulent kinetic energy dissipation. Using a series of numerical experiments in two idealized basin types under varying wind frequencies, we demonstrate that—in addition to the wave attractor ratio (de Carvalho Bueno et al., 2025)—the occurrence and efficiency of BBL separation as a driver of circulation and mixing depend critically on the ratio between the wind forcing period (σ_f) and the fundamental internal seiche period (T_{V1H1}). While previous studies hypothesized that periodic wind forcing could sustain boundary layer separation and associated transport processes through continuous system re-energization (de Carvalho Bueno et al., 2025), our results reveal a more nuanced dependence on this temporal scaling.

For wind forcing periods exceeding the fundamental internal seiche period ($\sigma_f/T_{V1H1} > 1$), our results demonstrate the generation of a non-resonant forced wave, consistent with previous laboratory findings (Boegman & Ivey, 2012). However, while in supercritical conditions this forced wave becomes modulated by a fundamental internal seiche (Figure 6c-d), the subcritical regime exhibits complete suppression of the fundamental wave mode. This suppression results from recurrent BBL

separation events that enhance energy dissipation rates by a factor of three compared to supercritical conditions (Figure 1), mirroring the behavior observed in single wind-pulse simulations.

Figure 6. Internal seiche dynamics and turbulent kinetic energy (TKE) dissipation under subcritical regime during periodic wind events. Panels a) and c) show time series (normalized by the wind period) of vertically integrated TKE dissipation and internal wave oscillations for wind periods of 5 h and 30 h, respectively. Panels b) and d) present the corresponding power spectral density (PSD) of internal wave oscillations. The gray line indicates the PSD under supercritical conditions at the respective wind frequency. The dotted line represents the 95% confidence level of the mean red noise spectrum, and the vertical red dashed line marks the fundamental internal seiche period (~15 h).

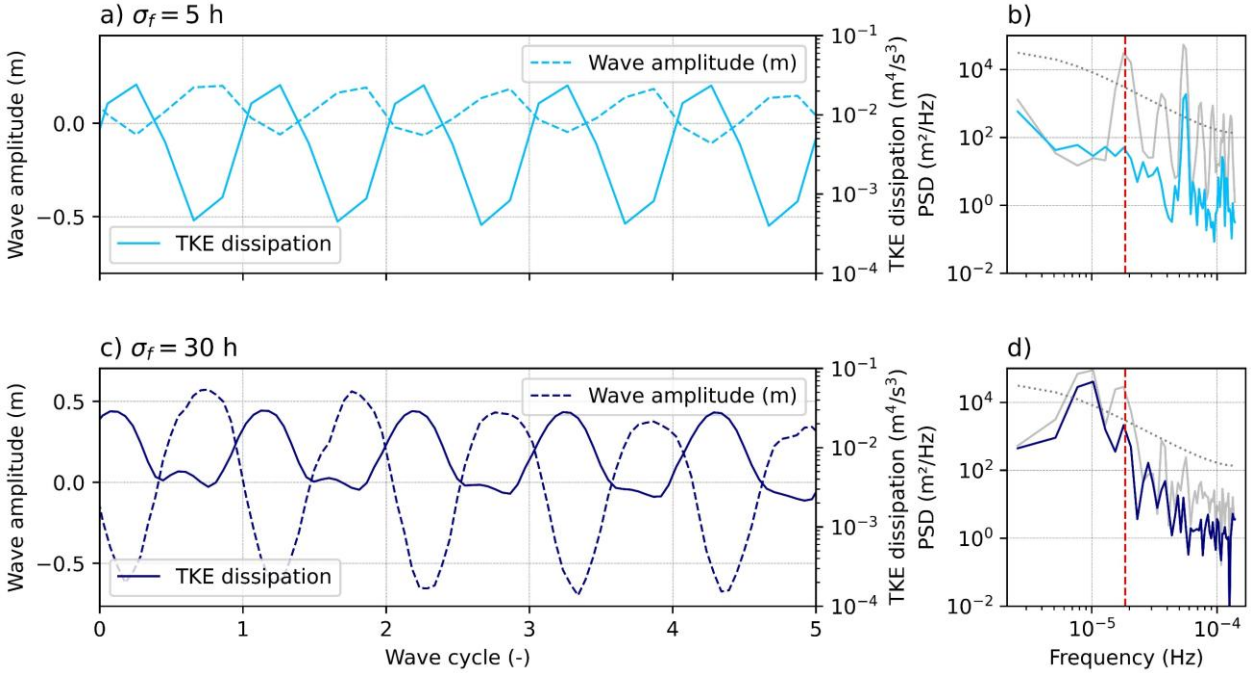

For wind forcing periods shorter than the fundamental internal seiche period ($\sigma_f / T_{V1H1} < 1$), complete separation of the BBL was partially inhibited. Under supercritical conditions, higher-mode internal seiches were generated (Figure 5a), consistent with previous observations (Boegman & Ivey, 2012). In contrast, subcritical conditions led to the formation of high-frequency internal wave (HFIW) packets with periods matching the wind forcing frequency. Although these HFIWs ultimately shoaled and broke near the sloping topography (Figure 5b), our analysis indicates TKE dissipation rates comparable to simulations under supercritical conditions.

The propagating waves generated under these conditions exhibited low Iribarren numbers (Boegman et al., 2005), resulting from the relatively steep topography compared to wave steepness. According to wave breaking theory, such conditions favor the formation of fission breakers, which are characterized by the splitting of waves into secondary wave trains upon interaction with the slope (Nakayama et al., 2019). Although fission breakers are generally associated with minimal localized mixing and enhanced offshore redistribution of wave energy (Masunaga et al., 2019), the specific TKE dissipation rates observed in this regime may be obscured by the grid resolution limitations of the field-scale numerical model (Aghsaee et al., 2010). These limitations may hinder the accurate representation of the small-scale turbulence associated with wave breaking. Therefore, future studies should aim to determine whether the observed dissipation patterns result from the model's inability to resolve the mechanics of breaking or from the inherent energy redistribution dynamics of fission-type wave breaking.

ACKNOWLEDGMENT

This work was carried out with the support of the coordination for the improvement of higher education personnel – Brazil (CAPES). Tobias Bleninger acknowledges the productivity stipend from the National Council for Scientific and Technological Development – CNPq, grant no. 312211/2020-1, call no. 09/2020. Rafael de Carvalho Bueno agradece a CAPES pela bolsa – código de financiamento 001.

REFERENCES

Aghsaee, P., Boegman, L., & Lamb, K. G. (2010). Breaking of shoaling internal solitary waves. *Journal of Fluid Mechanics*, *659*, 289–317. https://doi.org/10.1017/S002211201000248X

Amitai, Y., Strobach, E., Hamilton, D. P., Assouline, S., Nishri, A., & Zohary, T. (2024). Seiche-Induced Fish Kills in the Sea of Galilee—A Possible Explanation for Biblical Miracles? *Water Resources Research*, *60*(10). https://doi.org/10.1029/2024WR037894

Antenucci, J. P., & Imberger, J. (2003). The seasonal evolution of wind/internal wave resonance in Lake Kinneret. *Limnology and Oceanography*, *48*(5), 2055–2061. https://doi.org/10.4319/lo.2003.48.5.2055

Bernhardt, J., & Kirillin, G. (2013). Seasonal pattern of rotation-affected internal seiches in a small temperate lake. *Limnology and Oceanography*, *58*(4), 1344–1360. https://doi.org/10.4319/lo.2013.58.4.1344

Boegman, L., & Ivey, G. N. (2012). The dynamics of internal wave resonance in periodically forced narrow basins. *Journal of Geophysical Research: Oceans*, *117*(C11). https://doi.org/10.1029/2012JC008134

Boegman, L., Ivey, G. N., & Imberger, J. (2005). The degeneration of internal waves in lakes with sloping topography. *Limnology and Oceanography*, *50*(5), 1620–1637. https://doi.org/10.4319/lo.2005.50.5.1620

Chowdhury, M. R., Wells, M. G., & Howell, T. (2016). Movements of the thermocline lead to high variability in benthic mixing in the nearshore of a large lake. *Water Resources Research*, *52*(4), 3019–3039. https://doi.org/10.1002/2015WR017725

Cossu, R., & Wells, M. G. (2013). The interaction of large amplitude internal seiches with a shallow sloping lakebed: observations of benthic turbulence in Lake Simcoe, Ontario, Canada. *PloS One*, *8*(3), e57444. https://doi.org/10.1371/journal.pone.0057444

de Carvalho Bueno, R., Bleninger, T., Boehrer, B., & Lorke, A. (2023a). Physical mechanisms of internal seiche attenuation for non-ideal stratification and basin topography. *Environmental Fluid Mechanics*. https://doi.org/10.1007/s10652-023-09928-y

de Carvalho Bueno, R., Bleninger, T., Boehrer, B., & Lorke, A. (2023b). Physical mechanisms of internal seiche attenuation for non-ideal stratification and basin topography. *Environmental Fluid Mechanics*. https://doi.org/10.1007/s10652-023-09928-y

de Carvalho Bueno, R., Bleninger, T., & Lorke, A. (2020). Internal wave analyzer for thermally stratified lakes. *Environmental Modelling \& Software*. https://doi.org/10.1016/j.envsoft.2020.104950

de Carvalho Bueno, R., Bleninger, T., & Lorke, A. (2024). Transport and mixing induced by internal seiche destabilization on sloping bathymetry. *37th SIL International Congress on Limnology*.

de Carvalho Bueno, R., Bleninger, T., & Lorke, A. (2025). Internal seiche damping on sloping topography. *Submitted*.

Deltares. (2014). *Simulation of multi-dimensional hydrodynamic flows and transport phenomena, including sediments.*

Dorostkar, A., & Boegman, L. (2013). Internal hydraulic jumps in a long narrow lake. *Limnology and Oceanography*, *58*(1), 153–172. https://doi.org/10.4319/lo.2013.58.1.0153

Flood, B., Wells, M., Midwood, J. D., Brooks, J., Kuai, Y., & Li, J. (2021). Intense variability of dissolved oxygen and temperature in the internal swash zone of Hamilton Harbour, Lake Ontario. *Inland Waters*, 1–18. https://doi.org/10.1080/20442041.2020.1843930

Henderson, S. M., & Deemer, B. R. (2012). Vertical propagation of lakewide internal waves. *Geophysical Research Letters*, *39*(6), n/a-n/a. https://doi.org/10.1029/2011GL050534

Hingsamer, P., Peeters, F., & Hofmann, H. (2014). The consequences of internal waves for phytoplankton focusing on the distribution and production of Planktothrix rubescens. *PloS One*, *9*(8), e104359. https://doi.org/10.1371/journal.pone.0104359

Hodges, B. R., Imberger, J., Saggio, A., & Winters, K. B. (2000). Modeling basin-scale internal waves in a stratified lake. *Limnology and Oceanography*, *45*(7), 1603–1620. https://doi.org/10.4319/lo.2000.45.7.1603

Jarić, I., Říha, M., Souza, A. T., Rabaneda-Bueno, R., Děd, V., Gjelland, K. Ø., Baktoft, H., Čech, M., Blabolil, P., Holubová, M., Jůza, T., Muška, M., Sajdlová, Z., Šmejkal, M., Vejřík, L., Vejříková, I., & Peterka, J. (2022).

Influence of internal seiche dynamics on vertical movement of fish. *Freshwater Biology*, *67*(9), 1543–1558. https://doi.org/10.1111/fwb.13959

Laval, B., Imberger, J., Hodges, B. R., & Stocker, R. (2003). Modeling circulation in lakes: Spatial and temporal variations. *Limnology and Oceanography*, *48*(3), 983–994. https://doi.org/10.4319/lo.2003.48.3.0983

Lemmin, U. (1987). The structure and dynamics of internal waves in Baldeggersee. *Limnol. Oceanogr.*, *32*(1), 43–61. https://doi.org/10.4319/lo.1987.32.1.0043

Lin, S., Boegman, L., & Rao, Y. R. (2021). Characterizing spatial and temporal distributions of turbulent mixing and dissipation in Lake Erie. *Journal of Great Lakes Research*, *47*(1), 168–179. https://doi.org/10.1016/j.jglr.2020.11.014

Marti, C. L., & Imberger, J. (2006). Dynamics of the benthic boundary layer in a strongly forced stratified lake. *Hydrobiologia*, *568*(1), 217–233. https://doi.org/10.1007/s10750-006-0111-6

Masunaga, E., Arthur, R. S., & Fringer, O. B. (2019). Internal Wave Breaking Dynamics and Associated Mixing in the Coastal Ocean. In *Encyclopedia of Ocean Sciences* (pp. 548–554). Elsevier. https://doi.org/10.1016/B978-0-12-409548-9.10953-4

Mortimer, C. H. (1952). Water movements in lakes during summer stratification; evidence from the distribution of temperature in Windermere. *Philosophical Transactions of the Royal Society of London B: Biological Sciences*, *236*(635), 355–398. https://doi.org/10.1098/rstb.1952.0005

Nakayama, K., Sato, T., Shimizu, K., & Boegman, L. (2019). Classification of internal solitary wave breaking over a slope. *Physical Review Fluids*, *4*(1), 014801. https://doi.org/10.1103/PhysRevFluids.4.014801

Nielson, J. R., & Henderson, S. M. (2023). Periodic boundary layer separation and lateral intrusions observed above a sloping lakebed. *Limnology and Oceanography*, *68*(1), 26–39. https://doi.org/10.1002/lno.12246

Pannard, A., Beisner, B. E., Bird, D. F., Braun, J., Planas, D., & Bormans, M. (2011). Recurrent internal waves in a small lake: Potential ecological consequences for metalimnetic phytoplankton populations. *Limnology and Oceanography: Fluids and Environments*, *1*(1), 91–109. https://doi.org/10.1215/21573698-1303296

Plisnier, P.-D., Cocquyt, C., Cornet, Y., Poncelet, N., Nshombo, M., Ntakimazi, G., Nahimana, D., Makasa, L., & MacIntyre, S. (2023). Phytoplankton blooms and fish kills in Lake Tanganyika related to upwelling and the limnological cycle. *Journal of Great Lakes Research*, *49*(6), 102247. https://doi.org/10.1016/j.jglr.2023.102247

Roberts, D. C., Egan, G. C., Forrest, A. L., Largier, J. L., Bombardelli, F. A., Laval, B. E., Monismith, S. G., & Schladow, G. (2021). The setup and relaxation of spring upwelling in a deep, rotationally influenced lake. *Limnology and Oceanography*, *66*(4), 1168–1189. https://doi.org/10.1002/lno.11673

Spigel, R. H., & Imberger, J. (1980). The classification of mixed-layer dynamics of lakes of small to medium size. *Journal of Physical Oceanography*, *10*(7), 1104–1121. https://doi.org/10.1175/1520-0485(1980)010%3C1104:TCOMLD%3E2.0.CO;2

Stevens, C., & Imberger, J. (1996). The initial response of a stratified lake to a surface shear stress. *Journal of Fluid Mechanics*, *312*, 39–66. https://doi.org/10.1017/S0022112096001917

Stevens, C. L., & Lawrence, G. A. (1997). Estimation of wind-forced internal seiche amplitudes in lakes and reservoirs, with data from British Columbia, Canada. *Aquatic Sciences*, *59*(2), 115–134. https://doi.org/10.1007/BF02523176

Valerio, G., Pilotti, M., Lau, M. P., & Hupfer, M. (2019). Oxycline oscillations induced by internal waves in deep Lake Iseo. *Hydrology and Earth System Sciences*, *23*(3), 1763–1777. https://doi.org/10.5194/hess-23-1763-2019

Valipour, R., Boegman, L., Bouffard, D., & Rao, Y. R. (2017). Sediment resuspension mechanisms and their contributions to high-turbidity events in a large lake. *Limnology and Oceanography*, *62*(3), 1045–1065. https://doi.org/10.1002/lno.10485

Vilhena, L. C., Marti, C. L., & Imberger, J. (2013). The importance of nonlinear internal waves in a deep subalpine lake: Lake Iseo, Italy. *Limnology and Oceanography*, *58*(5), 1871–1891. https://doi.org/10.4319/lo.2013.58.5.1871

Wadzuk, B. M., & Hodges, B. R. (2009). Hydrostatic versus nonhydrostatic Euler-equation modeling of nonlinear internal waves. *Journal of Engineering Mechanics*, *135*(10), 1069–1080. https://doi.org/10.1061/(ASCE)0733-9399(2009)135:10(1069)

Welch, P. (1967). The use of fast Fourier transform for the estimation of power spectra: a method based on time averaging over short, modified periodograms. *IEEE Transactions on Audio and Electroacoustics*, *15*(2), 70–73. https://doi.org/10.1109/TAU.1967.1161901

Wüest, A., & Lorke, A. (2003). Small-scale hydrodynamics in lakes. *Annual Review of Fluid Mechanics*, *35*(1), 373–412. https://doi.org/10.1146/annurev.fluid.35.101101.161220